Indian J.Sci.Res. 17(2): 174 - 184, 2018 ISSN: 0976-2876 (Print)
ISSN: 2250-0138(Online)

ISLANDED AND GRID INTERCONNECTED OPERATION MODES OF PV SYSTEM

[1]Yellaiah Ponnam, [2]Ponnam Shiva Kumar, [3]Moota Sai Kiran
[1,2,3]Department of Electrical and Electronics Engineering, Aurora's Scientific Technological Research Academy, Hyderabad, Telangana, India

***Abstract*:** Photovoltaic (PV) is a method of generating electrical power by converting solar radiation into direct current electricity using semiconductors that exhibit the photovoltaic effect. Photovoltaic power generation employs solar panels composed of a number of solar cells containing a photovoltaic material. Materials presently used for photovoltaics include mono crystalline silicon, polycrystalline silicon, amorphous silicon, cadmium telluride, and copper/sulfide. PV panels tend to work much better in cold weather than in hot climates (except for amorphous silicon panels). The two types of stand-alone photovoltaic power systems are direct-coupled system without batteries and stand alone system with batteries and Grid-connected photovoltaic power systems are power systems energized by photovoltaic panels which are connected to the utility grid. Grid-connected photovoltaic power systems consist of Photovoltaic panels, MPPT, solar inverters, power conditioning units and grid connection equipment. Fuzzy Logic has two different meanings. In a narrow sense, Fuzzy Logic is a logical system, which is an extension of multivalve logic. However, in a wider sense Fuzzy Logic is almost synonymous with the theory of Fuzzy sets, a theory which relates to classes of objects with un sharp boundaries in which membership is a matter of degree. Here in this paper, intelligent control method uses a Fuzzy Logic Controller applied.

Keywords: Photovoltaic (PV) System, Grid-Connected Mode, Islanded Mode, Fuzzy Logic Controller.

I. Introduction

In recent years, the development of alternative energy sources has become a global priority, giving rise to intensive research about less environmentally polluting renewable sources. The installation of smaller and distributed power plants has been made possible due to changes in both the power system concept and the economy of scale. The proximity between production and consumption centers has regained importance [1], and distributed generation (DG) technologies have advanced greatly in recent years. One way to insert DG systems into an electrical network is through micro grids [2]. A micro grid can be defined as a combination of loads and micro sources that provide electric power to a local area. There are currently some important projects on micro grids around the world [3]–[6]. The operation of a micro grid offers distinct advantages to customers and utilities, i.e., improved energy efficiency, reduced environmental impact, and greater reliability. One of the most important features of micro grids is that they can independently operate in islanded mode without connection to the distribution system when power system faults or blackouts occur. Many commercial photovoltaic (PV) inverters work as a current source in grid-connected mode [7], [8].

The control of inverters has developed over time and is now highly efficient for this operational mode. Several works deal with the correct operation of inverters working in grid-connected and islanded modes. A possible solution is based on droop schemes. These schemes use P−Q strategies in the inverters to properly share the power delivered to the loads while avoiding critical communication lines. In [9] and [10], the inverters are controlled by means of droop schemes in both operational modes, so that no advantage is taken from control algorithms that inject the inverter output current in phase with the grid voltage (current source algorithms) developed for commercial grid-connected inverters. In [11], the inverter works as a current source by providing a constant current to the grid. The inverter detects when islanding occurs and changes to voltage source operation. The authors also propose a load-shedding algorithm for intentional islanding and a synchronization algorithm for grid reconnection. During islanding operation, the reference imposed on the inverter voltage controller has a fixed value, so that inverter parallelization for load power sharing is not possible.

Voltage sources connected by robust controller area network communications. However, this system requires a correctly operating communications bus, and this increases the cost. In other studies such as [13] and [14], reconfigurable control schemes are proposed, based on a very simple and effective type of control, namely, a multi loop linear proportional–integral (PI) control system. This method uses linear inner and outer PI control loops to regulate the system state variables. However, these papers do not clearly explain how inverters are parallelized when sharing the load power. There are multiple implementation options for energy storage. Some authors propose an energy storage independent from generators, as in [4], [15], and [16].

[1]Corresponding Author

Another option is to integrate storage and generation in a single system. Parallel integrated systems with a common dc bus are proposed in [17]–[19]. This dc bus has a fixed voltage, so that power converters for both generation and battery management are necessary to adequate the voltage and perform the maximum power point (MPP) tracking (MPPT) of the power sources. In [20], the proposed system is composed of a PV generator and a battery bank interconnected by means of a dc/dc converter. The inverter and the dc/dc converter share the same dc bus. The dc bus voltage is the same as the PV panel output voltage, which is imposed by an MPPT algorithm. This system has been designed for stand-alone applications. This paper shows a reconfigurable control scheme based on multi loop control in both operational modes. In grid-connection mode, the inverter is controlled as a current source in phase with the grid voltage. When the micro grid becomes isolated from the grid, the inverters change their control configuration, working as voltage sources and using a droop method [9], [21] – [23] to share the power demanded by the local loads. The droop method provides a good solution for parallelizing multiple inverters without using communications—as is detailed in the bibliography. The proposed PV energy system provides energy storage capability and allows maximizing the energy extracted from the PV panels in both operational modes. The system includes a parallel energy storage system composed of a battery bank and a dc/dc converter that ensures the MPPT of the PV source in islanded operation. Additionally, the proposed control reconfiguration is possible without dangerous transients for the inverter or the loads.

II. System Configurations

There are two main system configurations – stand-alone and grid-connected. As its name implies, the stand-alone PV system operates independently of any other power supply and it usually supplies electricity to a dedicated load or loads. It may include a storage facility (e.g. battery bank) to allow electricity to be provided during the night or at times of poor sunlight levels. Stand-alone systems are also often referred to as autonomous systems since their operation is independent of other power sources. By contrast, the grid-connected PV system operates in parallel with the conventional electricity distribution system. It can be used to feed electricity into the grid distribution system or to power loads which can also be fed from the grid.

It is also possible to add one or more alternative power supplies (e.g. diesel generator, wind turbine) to the system to meet some of the load requirements. These systems are then known as 'hybrid' systems.

Hybrid systems can be used in both stand-alone and grid-connected applications but are more common in the former because, provided the power supplies have been chosen to be complementary, they allow reduction of the storage requirement without increased loss of load probability. Figures(1-3) below illustrate the schematic diagrams of the three main system types.

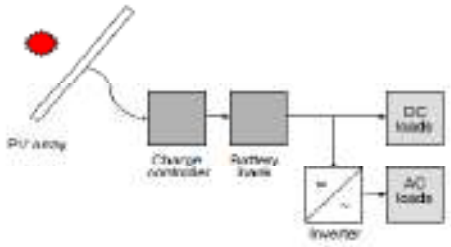

Fig 1.Schematic Diagram Of A Stand-Alone Photovoltaic System.

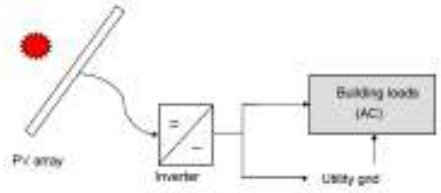

Fig.2. Schematic Diagram Of Grid-Connected Photovoltaic System.

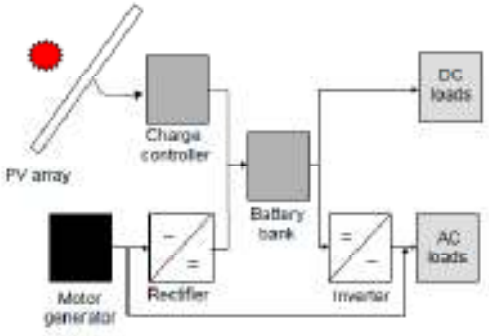

Fig.3. Schematic Diagram Of Hybrid System Incorporating A Photovoltaic Array And A Motor Generator (E.G. Diesel Or Wind).

A. PV modeling

A PV array consists of several photovoltaic cells in series and parallel connections. Series connections are responsible for increasing the voltage of the module whereas the parallel connection is responsible for increasing the current in the array. Typically a solar cell can be modeled by a current source and an inverted diode connected in parallel to it. It has its own series and parallel resistance. Series resistance is due to hindrance in the path of flow of electrons from n to p junction and parallel resistance is due to the leakage current.

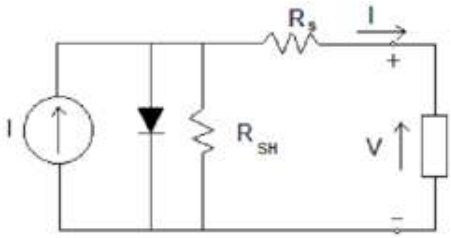

Fig.4. Single diode model of a PV cell

In this model we consider a current source (I) along with a diode and series resistance (R_s). The Shunt resistance (R_{SH}) in parallel is very high, has negligible effect and can be neglected.

The output current from the photovoltaic array is

$$\mathbf{I=I_{sc} - I_d}$$

$$\mathbf{I_d= I_o\ (e^{qV_d/kT} - 1)}$$

Where I_o is the reverse saturation current of the diode, q is the electron charge, V_d is the voltage Across the diode, k is Boltzmann constant (1.38 * 10^{-19}J/K) and T is the junction temperature in Kelvin (K)

$$\mathbf{I = I_{sc} - I_o\ (e^{qV_d/kT} - 1)}$$

Using suitable approximations,

$$\mathbf{I = I_{sc} - I_o\ (e^{q((V+IRs)/nkT)} - 1)}$$

Where , I is the photovoltaic cell current, V is the PV cell voltage, T is the temperature (in Kelvin) and n is the diode ideality factor In order to model the solar panel accurately we cause two diode model but in our project our scope of study is limited to the single diode model. Also, the shunt resistance is very high and can be neglected during the course of our study.

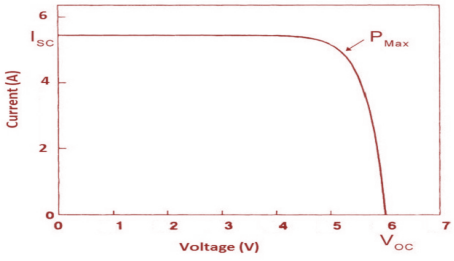

Fig.5. I-V characteristics of a solar panel

The I-V characteristics of typical solar cell areas shown in the Fig.5. When the voltage and the current characteristics are multiplied we get the P-V characteristics as shown in Fig.6. The point indicated as MPP is the point at which the panel power output is maximum.

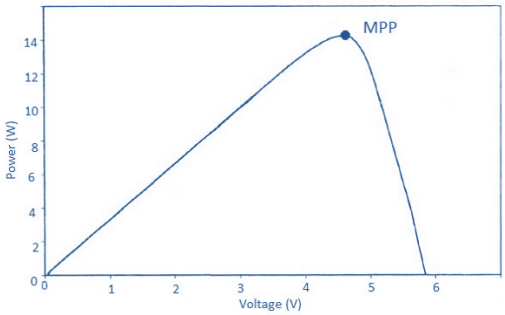

Fig.6. : P-V characteristics curve of photovoltaic cell

B. Maximum Power Point Tracking Algorithms

i. An overview of Maximum Power Point Tracking

A typical solar panel converts only 30 to 40 percent of the incident solar irradiation into electrical energy. Maximum power point tracking technique [24-25] is used to improve the efficiency of the solar panel. According to Maximum Power Transfer theorem, the power output of a circuit is maximum when the Thevenin's impedance of the circuit (source impedance) matches with the load impedance. Hence our problem of tracking the maximum power point reduces to an impedance matching problem. In the source side we are using a boost convertor connected to a solar panel in order to enhance the output voltage so that it can be used for different applications like motor load. By changing the duty cycle of the boost converter appropriately we can match the source impedance with that of the load impedance.

ii. Different MPPT techniques

There are different techniques used to track the maximum power point. Few of the most popular techniques are:

1) Perturb and observe (hill climbing method)
2) Incremental Conductance method
3) Fractional short circuit current
4) Fractional open circuit voltage
5) Neural networks
6) Fuzzy logic

The choice of the algorithm depends on the time complexity the algorithm takes to track the MPP, implementation cost and the ease of implementation.

iii. Implementation of MPPT using a boost converter

The system uses a boost converter to obtain more practical uses out of the solar panel. The initially low voltage output is stepped up to a higher level using the boost converter, though the use of the converter does tend to introduce switching losses. The block diagram shown in Fig.7.gives an overview of the required implementation.

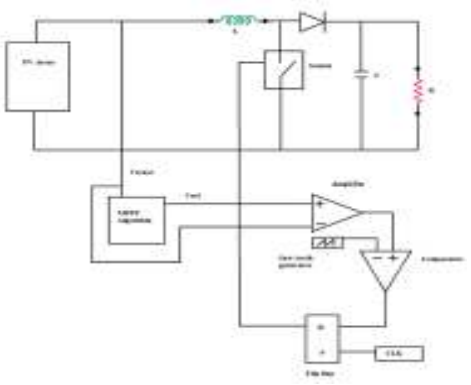

Fig.7. Requisite Implementation For MPPT System

III. PV System

The PV system under study, shown in Fig.8, includes a 3-kW full-bridge single-phase inverter and a bidirectional dc/dc converter. The dc/dc converter is connected to the dc link at the input of the inverter. The dc/dc converter manages the battery charge–discharge. The dc-link voltage V_{dc} is set by an MPP tracker[24] in both islanded mode and grid-connected mode. In islanded mode, the MPP tracker provides a reference voltage to the dc/dc converter, so that it regulates V_{dc}. In grid-connected mode, the MPP tracker delivers a reference voltage to the inverter, so that it can perform V_{dc} regulation. The MPPT is implemented by means of a perturb and observe algorithm. The MPP tracker defines the set point of the dc-link voltage to extract the maximum output power from the PV panel. The PV arrangement provides a dc-link voltage of around V_{dc}= 380V at the MPP, which is high enough to inject power to the grid (230Vrmsat 50 Hz) without a step-up transformer. To perform the simulations, the PV array has been modeled as a current source that is dependent on the incoming irradiance, inserting the I–V curves of the panels as a function of several irradiance levels by means of a table.

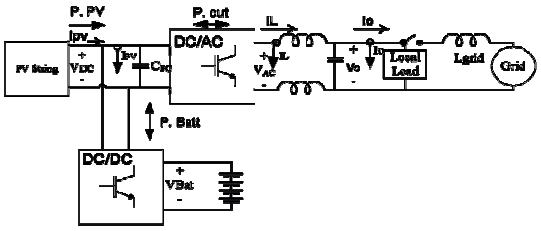

Fig.8. Block Diagram Of The PV System Under Study

A. Single-Phase Inverter

Fig.9. shows the scheme and the control structure of the inverter that has been implemented. A current-controlled H-bridge single-phase inverter with bipolar pulse width modulation has been chosen. This kind of inverter is common in grid-connected PV systems. The inverter is fed by a dc programmable source in which the I−V curve of a PV panel has been programmed to emulate an array of 14 series connected PV panels. Table I shows the electrical parameters of the PV inverter under study. The power of the inverter under study is 3 kW, with a switching frequency of 16 kHz.

B. Dc/Dc Converter

To improve the power management in the micro grid, backup energy storage is included. It consists of a battery bank connected to the inverter dc link by means of a two-quadrant bidirectional dc/dc converter. The main advantage of this configuration is that the dc/dc converter processes only a part of the generated power. This converter performs multiple functions.

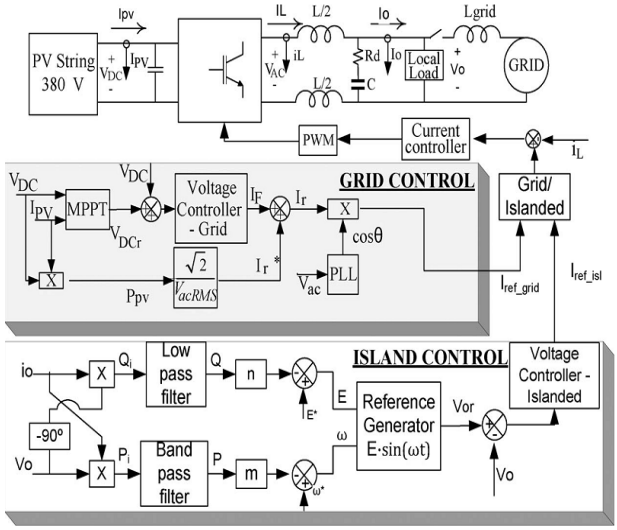

Fig .9. Control structure of the PV inverter.

Table I Electrical Parameters Of The Inverter Under Study

Parameter	Value
Power injected from the PV panels ($P_{pv\,MPP}$)	*3 kW*
DC-link voltage al the MPP ($V_{DC\,MPP}$)	*380 V*
Inverter output voltage (V_{O_RMS})	*230 V_{RMS} ±10%*
Fundamental frequency of the inverter output (f_g)	*50 Hz*
Inverter inductance (L)	*2.7 mH*
DC-link capacitor (C_{DC})	*2mF*
Inverter output capacitor (C)	*4.5 μF*
Damping resistance (R_d)	*5 Ω*
Inverter switching frequency ($f_{s\,inv}$)	*16 kHz*

It serves as a battery charge regulator in grid-connected operation and a boost converter to deliver energy from the batteries to the inverter when the PV source has insufficient power to feed the local loads in islanded operation. In islanded mode, the most favorable operating

condition occurs when the load power and the PV extracted power agree, i.e., when the dc/dc converter does not process power. Fig.10. shows the simplified dc/dc converter power stage and its control structure. Table II shows the electrical parameters of the dc/dc converter under study. The islanded and grid-connected operational modes are explained in the following sections.

C. Dynamic Analysis

The inverter switches from grid-connected mode to islanded mode by selecting between two current references: I_{ref_grid} and I_{ref_isl}, as shown in Fig.9. The method described is used to detect the islanding condition. A stability analysis of the converters is shown for both operation modes.

D.PV Power System Working in Grid-Connected Mode

In grid-connected mode, the dc-link voltage (V_{dc}) control is performed by the inverter, following a reference provided by the MPPT algorithm. A PI controller (voltage controller-grid element in Fig.9.) is used for the inverter voltage loop in this operational mode. A feed forward term I_r, expressed by (1), is added to the output of the PI dc-link voltage controller I_F, yielding the amplitude of the current loop reference I_r.

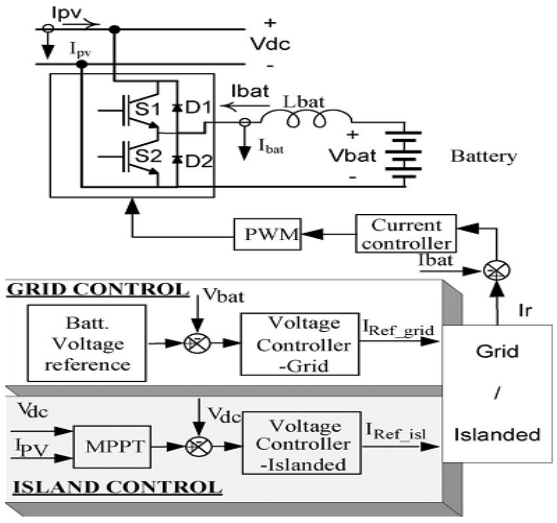

Fig.10. DC–DC converter schematic and control structure.

Table II .Electrical Parameters Of The DC–DC Converter

Parameter	Values
Peak power extracted from the batteries	3 kW
DC-link voltage ($V_{DC\ MPP}$)	380 V
Battery bank voltage (V_{Bat})	220 V
Converter inductance (L_{bat})	7 mH
Converter switching frequency ($f_{s\ dcdc}$)	16 kHz

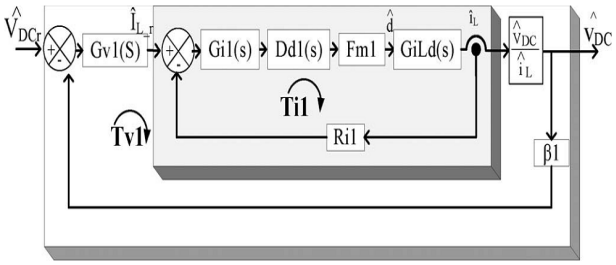

Fig.11. Inverter control loops in grid-connected operation.

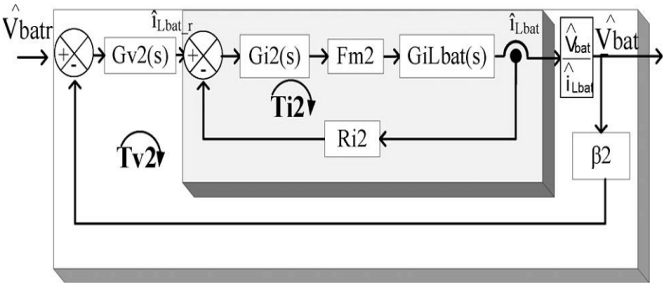

Fig.12. DC/DC converter control loops in grid-connected operation.

The term I^*_r is derived from the active power that is being delivered by the PV source

$$I_r^* = \frac{P_{PV} \cdot \sqrt{2}}{V_{acrms}}$$

The amplitude I_r is multiplied by the term cosθ, provided by a phase-locked loop (dqPLL) operating from the grid voltage. The dqPLL is implemented using the synchronous rotating reference frame technique. The angle θ is that of the fundamental component of the grid voltage. The current controller was implemented by means of a harmonic compensator in order to comply with the standard IEEE 929-2000 in terms of both the current total harmonic distortion (THD_i) and the individual limits of harmonics. Figs.11. and fig.12. show the control loop block diagrams in grid connected operational mode for the inverter and the dc/dc converter, respectively.

For this reason, it is necessary to find the reference of the inverter output voltage (V_{or} in Fig.9.) in terms of the active

power and reactive power consumed by the loads. The method used to determinate this voltage reference is the droop method as shown in Fig.. In the system under study, an only PV inverter has been considered, with the goal of our research being the change from grid-connected mode to islanded mode with a battery as additional energy storage, not the droop method in itself. As only one inverter in islanded mode has been studied, the droop method is not necessary. Nevertheless, the inverter control has been developed to work in a micro grid environment, in parallel with other inverters. Therefore, the analysis and the experimental results have been obtained with the full algorithm working (droop + inverter current and voltage loops). The voltage reference of the inverter output voltage controller (voltage controller-islanded element in Fig.9.) is synthesized by means of the droop scheme. In islanded operation mode, the dc-link voltage is controlled by the battery-side dc–dc converter following a reference set by the MPPT algorithm. Figs.13. and 14 show the inverter and dc/dc converter control loops for islanded operation, respectively. In Table V, the transfer functions of interest for the control of the system in islanded mode are summarized. The term $Z_L(s)$ stands for the impedance of the local load in islanded mode. Table VI shows the expressions of the chosen regulators for both the inner current loop and the outer voltage loop, along with the corresponding crossover frequencies (f_C) and PMs for the inverter and dc/dc converter in islanded mode.

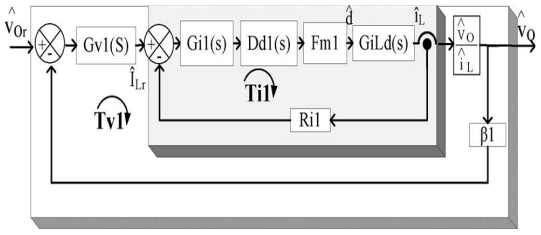

Fig.13. Inverter control loops in islanded operation.

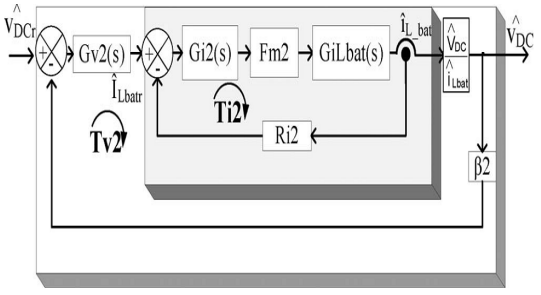

Fig.14. DC/DC converter control loops in islanded operation.

To avoid abrupt transitions from one operation mode to another, it is necessary to equalize the initial conditions of the current controllers of both the inverter and the dc/dc converter before the change. It should be pointed out that, when switching from one mode to the other, the same transfer functions of the current controllers are used .

E. Construction of Fuzzy Controller

Fig.15. shows the internal structure of the control circuit. The control scheme consists of Fuzzy controller, limiter, and three phase sine wave generator for reference current generation and generation of switching signals. The peak value of reference currents is estimated by regulating the DC link voltage. The actual capacitor voltage is compared with a set reference value. The error signal is then processed through a Fuzzy controller, which contributes to zero steady error in tracking the reference current signal. A fuzzy controller converts a linguistic control strategy into an automatic control strategy, and fuzzy rules are constructed by expert experience or knowledge database. Firstly, input voltage V_{dc} and the input reference voltage V have been placed of the angular velocity to be the input variables of the fuzzy logic controller. Then the output variable of the fuzzy logic controller is presented by the control Current Imax. To convert these numerical variables into linguistic variables, the following seven fuzzy levels or sets are chosen as: NB (negative big), NM (negative medium), NS (negative small), ZE (zero), PS (positive small), PM (positive medium), and PB (positive big) as shown in Fig.10.

The fuzzy controller is characterized as follows:

- Seven fuzzy sets for each input and output;
- Fuzzification using continuous universe of discourse;
- Implication using Mamdani's “min“ operator;
- De-fuzzification using the “centroid“ method.

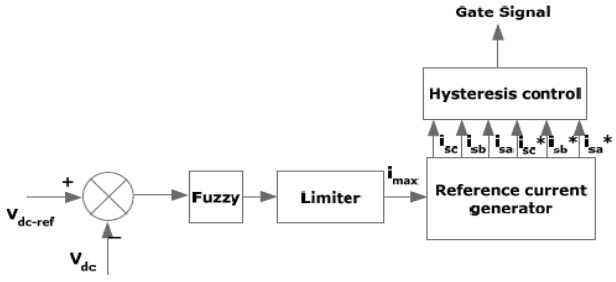

Fig.15.. Conventional fuzzy controller

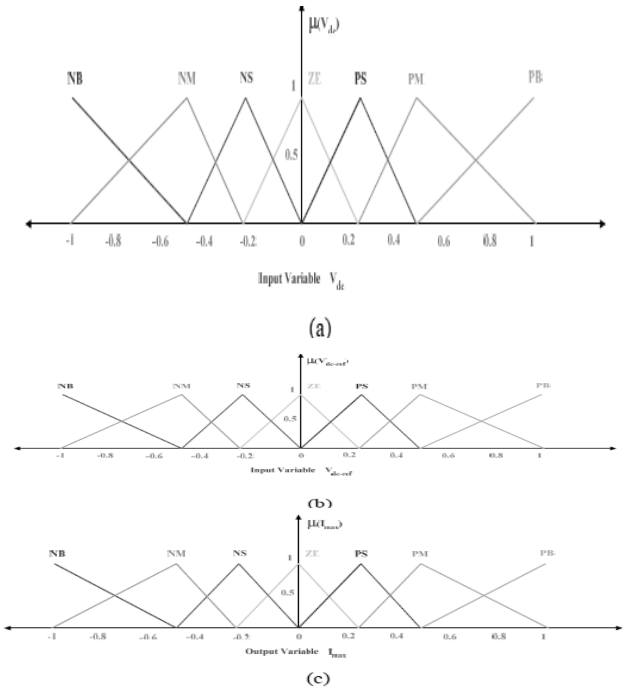

Fig.16. (a) Input Vdc normalized membership function; (b) Input Vdc-ref Normalized Membership Function; (c) Output Imax Normalized Membership Function.

Fuzzy Rule Base: the elements of this rule base table are determined based on the theory that in the transient state, large errors need coarse control, which requires coarse input/output variables; in the steady state, small errors need fine control, which requires fine input/output variables. Based on this the elements of the rule table are obtained as shown in Table-IV, with V_{dc} and $V_{dc\ ref}$

Table-IV Fuzzy rule base

V_{dc-ref} / V_{dc}	NB	NM	NS	Z	PS	PM	PB
NB	NB	NB	NB	NB	NM	NS	Z
NM	NB	NB	NB	NM	NS	Z	PS
NS	NB	NB	NM	NS	Z	PS	PM
Z	NB	NM	NS	Z	PS	PM	PB
PS	NM	NS	Z	PS	PM	PB	PB
PM	NS	Z	PS	PM	PB	PB	PB
PB	Z	PS	PM	PB	PB	PB	PB

F. SIMULIK Modeling And Results

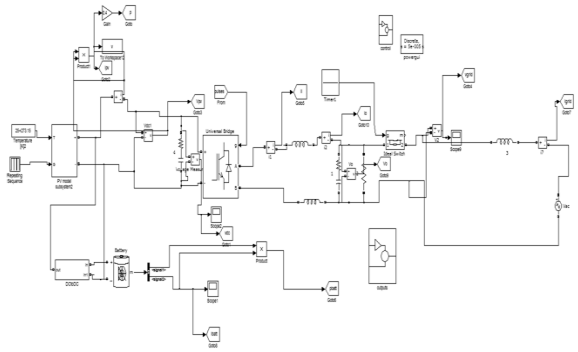

Fig.17. Simulation of grid-connected mode

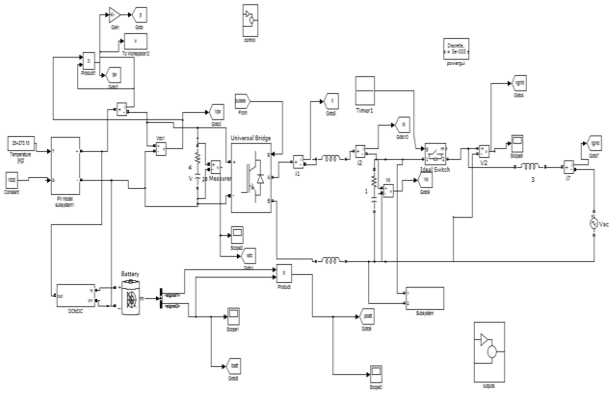

Fig.18. Simulation of islanded mode

Figure.17 and 18 shows the simulation diagrams grid connected mode and of Islanded mode: resistive load variation(1kW-1.7kW)In islanded mode at a constant P_{pv}=1.8 kW and Inverter output power decreases or increases depending on the load power, whereas the PV output power and the DC link voltage remains constant with PI Controller.

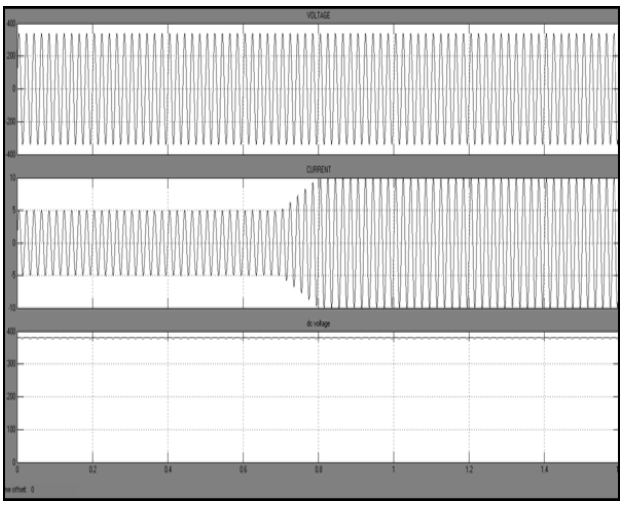

Fig.19. Simulation results of proposed system with an irradiance variation followed by a battery charge

variation in grid-connected mode.

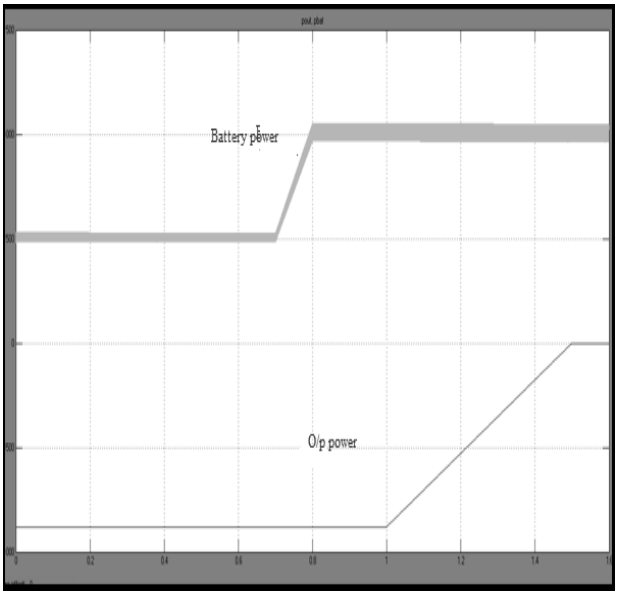

Fig.20.Battery charge variation in grid connected mode.

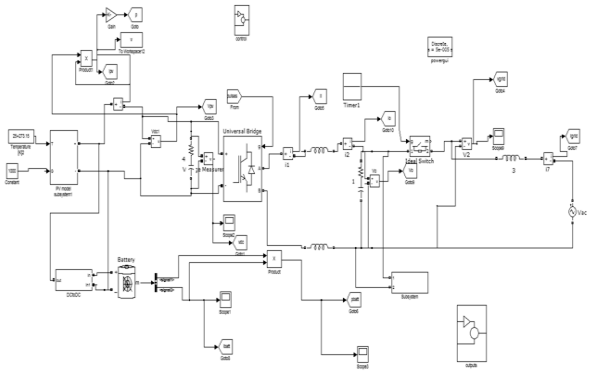

Fig.21 Transition from islanded mode to grid connected mode

Figure .21.shows the simulation of a transition from islanded mode to grid connected mode of the synchronization of the Inverter output voltage and grid voltage with PI controller and THD is 3.78%.

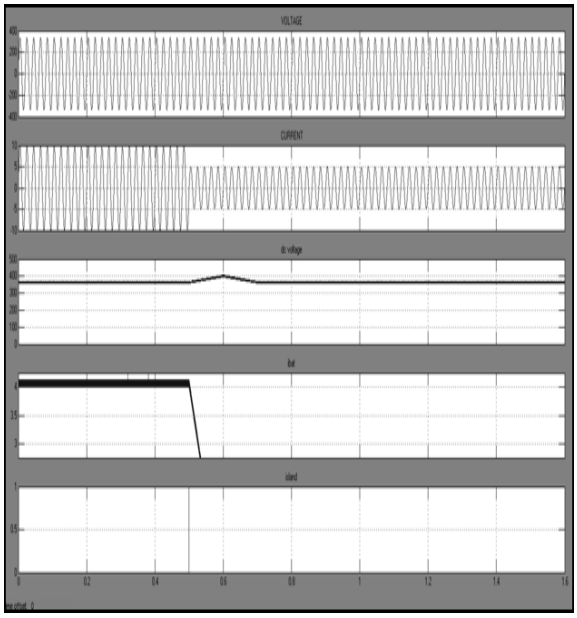

Fig: 22.Transition from islanded mode to grid-connected mode.

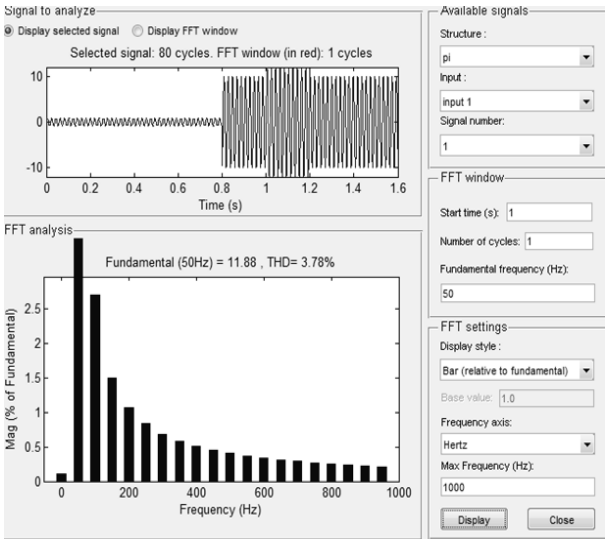

Fig:23. THD of islanded mode to grid connected mode with PI controller

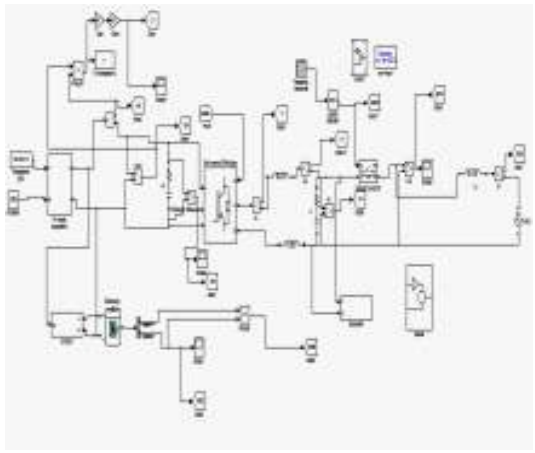

Fig:24. Transition from islanded mode to grid-connected mode with fuzzy controller

Figure.24. shows the simulation of a transition from islanded mode to grid connected mode of the synchronization of the Inverter output voltage and grid voltage with Fuzzy controller and THD is 1.78%.

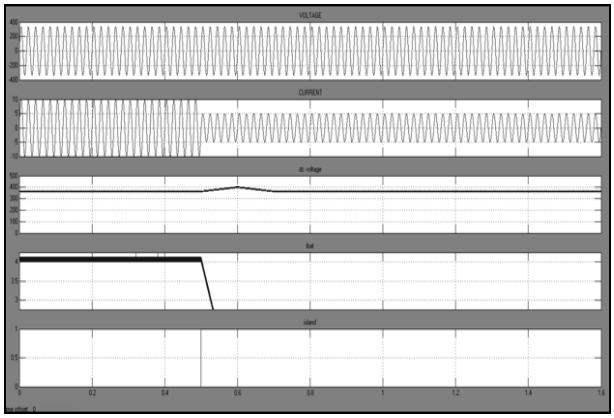

Fig. 25 Transition from islanded mode to grid-connected mode.

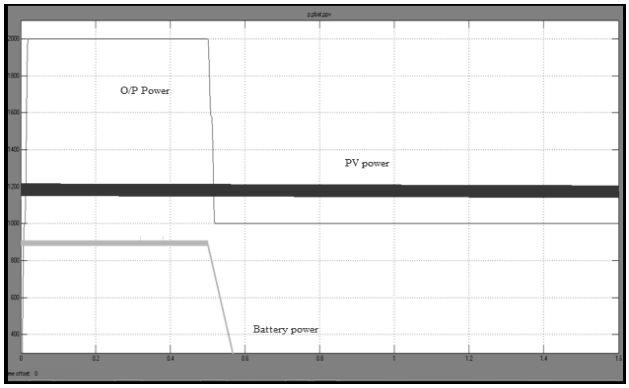

Fig: 26. Fuzzy controller with islanded mode to grid-connected.

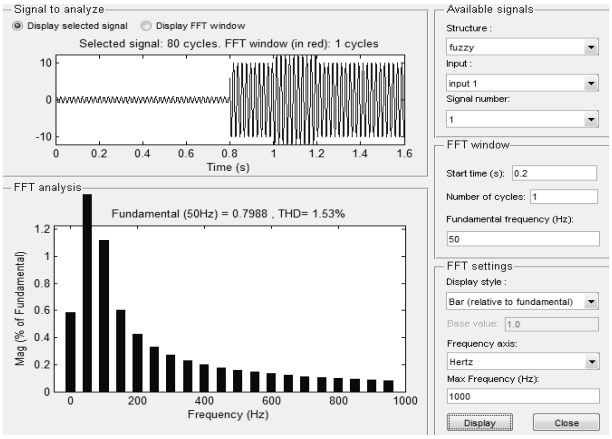

Fig: 27. THDV of islanded mode to grid connected mode with fuzzy controller.

IV. Conclusion

The system is based on a battery-side dc/dc converter connected to the dc link of the PV inverter. The control of the dc-link voltage is performed by the dc/dc converter in islanded operation and by the inverter in grid connected mode. The MPPT algorithm provides the dc-link voltage reference for either of the power converters. Only a part of the generated power is processed by the dc/dc converter. The power flow in the batteries and their charge level are controlled by the dc/dc converter.

The transition between grid-connected and islanded modes and vice versa is implemented by means of a reconfiguration of controllers. In grid-connection mode, the inverter is controlled as a current source in phase with the grid voltage. When the inverter becomes isolated from the grid, the inverter changes its control configuration, working as a voltage source and using the droop method to feed the local loads. The batteries provide the supplementary power to the loads if the PV available power is insufficient.

The MATLAB/SIMULINK circuit of the proposed system with Fuzzy logic based MPPT. In this the PV system is connected to the DC-DC converter to extract maximum power. The DC-DC converter operates according to MPPT. Simulation results of proposed system with an irradiance variation followed by a battery charge variation in grid-connected mode.

References

[1] "Renewable 2009, Global Status Report," World watch Inst., Washington, DC, 2009.

[2] H. B. Puttgen, P. R. Mac Gregor, F. C. Lambert, "Distributed generation: Semantic hype or the dawn of a new era?" *IEEE Power Energy Mag.*,vol. 1, no. 1, pp. 22–29, Jan./Feb. 2003.

[3] Y. Zhu, Z. Yin, and J. Tian,"Micro grids based on dc energy pool," in *Proc. IEEE ENERGY*, Nov. 17–18, 2008, pp. 1–2.

[4] B. Belvedere, M. Bianchi, A. Borghetti, and M. Paolone, "A microcontroller-based automatic scheduling system for residential microgrids," in *Proc. IEEE Bucharest PowerTech*, Jun. 2009, pp. 1–6.

[5] C. Sudipta, W. Manoja, and M. Godoy "Distributed intelligent energy management system for a single-phase high-frequency ac microgrid," *IEEE Trans. Ind. Electron.*, vol. 54, no. 1, pp. 97–109, Feb. 2007.

[6] T. Selim, C. Ozansoy, and A. Zayegh, "Recent developments in microgrids and example cases around the world—A review," *Renew. Sustain. Energy Rev.*, vol. 15, no. 8, pp. 4030–4041, Oct. 2011.

[7] Y. M. Chen, H. Wu, Y. C. Chen, K. Y. Lee, and S. S. Shyu, "The ac line current regulation strategy for the grid-connected PV system," *IEEE Trans. Power Electron.*, vol. 25, no. 1, pp. 209–218, Jan. 2010.

[8] M. Ciobotaru, R. Teodorescu, and F. Blaabjerg, "Control of single-stage single-phase PV inverter, power electronics and applications," in *Proc. Eur. Conf. Power Electron. Appl.*, 2005, p. 10.

[9] J. M. Guerrero, J. C. Vasquez, J. Matas, M. Castilla, and L. G. de Vicuna, "Control strategy for flexible microgrid based on parallel line-interactive UPS systems," *IEEE Trans. Ind. Electron.*, vol. 56, no. 3, pp. 726–736, Mar. 2009.

[10] K. Jaehong, J. M. Guerrero, P. Rodriguez, R. Teodorescu, and N. Kwanghee, "Mode adaptive droop control with virtual output impedances for an inverter-based flexible ac microgrid," *IEEE Trans. Power Electron.*, vol. 26, no. 3, pp. 689–701, Mar. 2011.

[11] I. J. Balaguer, L. Qin, Y. Shuitao, U. Supatti, and F. Z. Peng, "Control for grid-connected and intentional islanding operations of distributed power generation," *IEEE Trans. Ind. Electron.*, vol. 58, no. 1, pp. 147–157, Jan. 2011.

[12] C. L. Chen, Y. Wang, J. S. Lai, Y. S. Lee, and D. Martin, "Design of parallel inverters for smooth mode transfer microgrid applications," *IEEE Trans. Power Electron.*, vol. 25, no. 1, pp. 6–15, Jan. 2010.

[13] K. Hyosung, Y. Taesik, and C. Sewan, "Indirect current control algorithm for utility interactive inverters in distributed generation systems," *IEEE Trans. Power Electron.*, vol. 23, no. 3, pp. 1342–1347, May 2008.

[14] M. A. Hassan and M. A. Abido, "Optimal design of microgrids in autonomous and grid-connected modes using particle swarm optimization," *IEEE Trans. Power Electron.*, vol. 26, no. 3, pp. 755–769, Mar. 2011.

[15] I. Serban and C. Marinescu, "A look at the role and main topologies of battery energy storage systems for integration in autonomous microgrids," in *Proc. 12th Int. Conf. OPTIM*, May 20–22, 2010, pp. 1186–1191.

[16] I. Serban and C.Marinescu, "Active power decoupling circuit for a singlephase battery energy storage system dedicated to autonomous microgrids," in *Proc. IEEE ISIE*, Jul. 4–7, 2010, pp. 2717–2722.

[17] M. A. Sofla and L. Wang, "Control of dc–dc bidirectional converters for interfacing batteries in microgrids," in *Proc. IEEE/PESPSCE*, Mar. 20–23, 2011, pp. 1–6.

[18] I. B. Song, D. Y. Jung, Y. H. Ji, S. C. Choi, S. W. Lee, and C. Y. Won, "A residential 10 kWh lithium-polymer battery energy storage system," in *Proc. 8th IEEE ICPE ECCE Asia*, May 30–Jun. 3 2011, pp. 2625–2630.

[19] G. Y. Choe, J. S. Kim, B. K. Lee, C. Y. Won, and T. W. Lee, "A bidirectional battery charger for electric vehicles using photovoltaic PCS systems," in *Proc. IEEE VPPC*, Sep. 1–3, 2010, pp. 1–6.

[20] R. Gules, J. De Pellegrin Pacheco, H. L. Hey, and J. Imhoff, "A maximum power point tracking system with parallel connection for PV stand-alone applications," *IEEE Trans. Ind. Electron.*, vol. 55, no. 7, pp. 2674–2683, Jul. 2008.

[21] J. C. Vasquez, J. M. Guerrero, A. Luna, P. Rodriguez, and R. Teodorescu, "Adaptive droop control applied to voltage-source inverters operating in grid-connected and islanded modes," *IEEE Trans. Ind. Electron.*, vol. 56, no. 10, pp. 4088–4096, Oct. 2009.

[22] J. M. Guerrero, J. Matas, L. G. de Vicuna, M. Castilla, and J. Miret, "Wireless-control strategy for parallel operation of distributed-generation inverters," *IEEE Trans. Ind. Electron.*, vol. 53, no. 5, pp. 1461–1470, Oct. 2006.

[23] W. Yao, M. Chen, J. Matas, J. M. Guerrero, and Z. M. Qian, "Design and analysis of the droop control method for parallel inverters considering the impact of the complex impedance on the power

sharing," *IEEE Trans. Ind. Electron.*, vol. 58, no. 2, pp. 576–588, Feb. 2011.

[24] T. Esram and P. L. Chapman, "Comparison of photovoltaic array maximum power point tracking techniques," *IEEE Trans. Energy Conv.*, vol. 22, no. 2, pp. 439–449, Jun. 2007.

[25] N. Femia, G. Petrone, G. Spagnuolo, and M. Vitelli, "A technique for improving P&O MPPT performances of double-stage grid-connected photovoltaic systems," *IEEE Trans. Ind. Electron.*, vol. 56, no. 11, pp. 4473–4482, Nov. 2009.

[26] N. Mohan, T. Undeland, and W. Robbins, *Power Electronics: Converters, Applications, and Design*. Hoboken, NJ: Wiley, 1995.

[27] M. Liserre, F. Blaabjerg, R. Teodorescu, and Z. Chen, "Power converters and control of renewable energy systems," in *Proc. ICPE*, Busan, Korea, Invited paper.

[28] D. Velasco, C. Trujillo, G. Garcera, and E. Figueres, "An active antiislanding method based on phase-PLL perturbation," *IEEE Trans. Power Electron.*, vol. 26, no. 4, pp. 1056–1066, Apr. 2011.

[29] M. Ciobotaru, R. Teodorescu, and F. Blaabjerg, "A new single-phase PLL structure based on second order generalized integrator," in *Proc. IEEE PESC*, Jeju, Korea, 2006, pp. 1511–1516.

[30] M. Liserre, A. Timbus, R. Teodorescu, and F. Blaabjerg, "Synchronization methods for three phase distributed power generation systems. An overview and evaluation," in *Proc. PESC*, Recife, Brazil, 2005,pp. 2474–2481.

[31] N. Femia, G. Petrone, G. Spagnuolo, and M. Vitelli, "Optimization of perturb and observe maximum power point tracking method," *IEEE Trans. Power Electron.*, vol. 20, no. 4, pp. 963–973, Jul. 2005.

[32] *IEEE Recommended Practice for Grid Interface of Photovoltaic (PV) Systems*, IEEE Std. 929, 2000